

Figure 4. Dependence of k_1 on temperature at different pressures of N_2 . Experimental points: (O) this work at 25 Torr; (X) this work at 50 Torr; (*) this work at 100 Torr; (■) ref 5 at 100 Torr; (▲) ref 5 at 700 Torr. The lines drawn at each pressure come from a fit of this complete data set to eq I-III.

The assignment of a fixed value for F_c does not precisely follow the Troe³ theory to the letter since F_c has a temperature dependence of its own, although calculations by Patrick and Golden⁷ indicate only a small change in F_c (from 0.72 to 0.61) for this reaction between 200 and 300 K. While the analysis performed in our room temperature studies demonstrated a significant dependence of k_∞ on F_c , this dependence was greatest for F_c values below 0.5. In addition, only a small change in k_0 was observed for a nearly twofold variation in F_c . Thus, adoption of the 0.6 value for F_c chosen by the NASA Panel for Data Evaluation does not result in k_0 and k_∞ values far removed from the "true" low-

and high-pressure limiting rate constants.

The room temperature falloff curves for this composite data base are shown in Figure 3. With these values for $k_{0,N_2}(300K)$ and $k_\infty(300K)$, the temperature-dependent N_2 data from both laboratories were then fit to eq I-III by using a weighted nonlinear least-squares analysis. This treatment yielded

$$n = 3.2 \pm 0.4$$

$$m = 1.4 \pm 1.0$$

where the uncertainties expressed are two standard deviations from the least-squares fit. Thus the temperature dependence of the falloff parameters can be expressed as

$$k_{0,N_2}(T) = 1.8 \times 10^{-31} \{T/300\}^{-(3.2 \pm 0.4)} \text{ cm}^6 \text{ molecule}^{-2} \text{ s}^{-1}$$

$$k_\infty(T) = 4.7 \times 10^{-12} \{T/300\}^{-(1.4 \pm 1.0)} \text{ cm}^3 \text{ molecule}^{-1} \text{ s}^{-1}$$

The composite data set is shown with the computed curves in Figure 4. As can be seen there is excellent agreement between the 100 Torr data of the present study and that of ref 5 and the computed curves are not biased toward either end of the pressure or temperature ranges. The temperature dependencies determined are only moderately different from those currently recommended for atmospheric modeling⁶ which, as mentioned, are based on a limited data set coupled with theoretical computations. These differences are most evident in the low-pressure/high-temperature region and are not very significant under stratospheric conditions.

Acknowledgment. The research described in this manuscript was conducted at the National Bureau of Standards with the support of the National Aeronautics and Space Administration (Agreement W-15,816).

Registry No. HO_2 , 3170-83-0; NO_2 , 10102-44-0.

Kinetic Control in Two-Electron Homogeneous Redox Electrocatalysis. Reduction of Monohalobiphenyls

James V. Arena and James F. Rusling*

Department of Chemistry (U-60), University of Connecticut, Storrs, Connecticut 06268

(Received: October 10, 1986; In Final Form: December 29, 1986)

Kinetic control of the two-electron electrocatalytic dehalogenation of monohalobiphenyls to biphenyl was elucidated by analyzing voltammetric data with expanded-grid digital simulation/nonlinear regression. The method involves comparing goodness of fit of limiting and mixed kinetic simulation models to the data and is applicable to second-order conditions. The rate-determining step in the dehalogenations was confirmed as electron transfer between the electrochemically generated phenanthridine anion radical and 4-chloro- (4-CB) and 4-bromobiphenyl (4-BB), rather than decomposition of the halobiphenyl anion radical. Rate constants for this step of $(1.42 \pm 0.12) \times 10^3 \text{ M}^{-1} \text{ s}^{-1}$ for 4-CB and $(5.1 \pm 1.8) \times 10^4 \text{ M}^{-1} \text{ s}^{-1}$ for 4-BB showed considerably improved precision (and accuracy in the latter case) over rate constants obtained under pseudo-first-order conditions, where the catalytic current had to be extracted from large currents for direct reduction of excess substrate. The simulation/regression method is general for two-electron homogeneous electrocatalytic reactions following similar mechanisms. Synthetic data were used to show that, for systems under mixed kinetic control, rate constants for both homogeneous electron transfer and decomposition of the haloaromatic anion radical can be estimated simultaneously.

Introduction

Reductive dehalogenation of mono- and polyhalobiphenyls (e.g., PCB's) in *N,N*-dimethylformamide (DMF) is catalyzed at mercury and glassy carbon electrodes by soluble organic redox couples¹⁻⁴ which accept electrons rapidly from the cathode. These

reactions are examples of homogeneous redox electrocatalysis, in which the electrochemically generated anion radicals of the catalyst transfer electrons to the PCB's, yielding biphenyl by a stepwise reduction of carbon-halogen bonds. These two-electron dehalogenations were studied for five halobiphenyl substrates and fifteen catalysts⁴ under conditions pseudo-first order in catalyst. Loss of the first halogen follows¹⁻⁴ Scheme I, similar to that for ha-

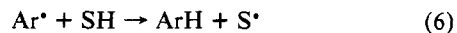
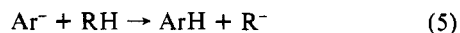
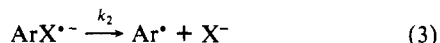
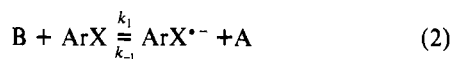
(1) Connors, T. F.; Rusling, J. F. *J. Electrochem. Soc.* **1983**, *130*, 1120-1121.

(2) Rusling, J. F.; Connors, T. F. *Anal. Chem.* **1983**, *55*, 776-781.

(3) Connors, T. F.; Rusling, J. F. *Chemosphere* **1984**, *13*, 415-420.

(4) Connors, T. F.; Rusling, J. F.; Owlia, A. *Anal. Chem.* **1985**, *57*, 170-174.

SCHEME I



lobenzenes and halopyridines.⁵ The first step is fast transfer of an electron from the electrode to catalyst A (eq 1). The rate-determining step (rds) for the halobiphenyls under the conditions used was homogeneous electron transfer from catalyst anion radical (B) to substrate (eq 2). Considering standard potentials of A and ArX,⁴ the forward reaction in eq 2 is thermodynamically unfavorable, and the overall reaction is driven by rapid cleavage⁴⁻⁶ of the intermediate halobiphenyl anion radical in eq 3. Additional fast electron transfer⁷ and chemical steps (eq 4-6), where RH = proton donor and SH = solvent or electrolyte, lead to nearly quantitative formation of biphenyl.^{1,3} If H-atom abstraction (eq 6) is significant, S[•] is reduced to retain two-electron stoichiometry.

We previously obtained the rate constant k_1 using linear-sweep voltammetry (LSV) with a large excess of substrate. At relatively low scan rates, these pseudo-first-order conditions forced the measured current to be under pure kinetic control of the homogeneous electron transfer in eq 2. This gives rise to a sigmoid current-potential ($I-E$) curve, described by a simple closed form relation between I and E .² Because the irreversible voltammetric curve for direct reduction of excess substrate overlapped the catalytic current for the reaction in Scheme I, nonlinear regression was used to extract the catalytic current,⁴ the limiting value of which is proportional to $k_1^{1/2}$. The precision of k_1 decreased as the standard potential of the catalyst became closer to the irreversible reduction peak of the substrate.² However, the pseudo-first-order method allowed determination of k_1 by analysis of the entire current-potential ($I-E$) curve and gave slightly better precision than regression analysis of data from which the non-catalytic contribution had been subtracted.

Improved precision and accuracy in k_1 should be afforded by a method to analyze catalytic $I-E$ data under second-order conditions. With comparable concentrations of catalyst and substrate, the contribution to the current from direct reduction of substrate should be negligible in many systems. Moreover, by raising the catalyst concentration it is sometimes possible to shift kinetic control to eq 3, enabling determination of k_2 if k_1 is known.^{5,8,9} On the other hand, closed form expressions relating I to E are not available for second-order redox electrocatalysis. We recently described¹⁰ a method of analyzing electrochemical data which used nonlinear regression of data onto expanding space grid digital simulation models. This method was successfully applied to obtain k_1 from voltammetric data for the reduction of 4-chlorobiphenyl with phenanthridine as catalyst, using the ad hoc assumption that eq 2 was the rds. In this paper, we extend the method to the

problem of elucidating the nature of kinetic control in reactions following Scheme I. In addition to improving precision in rate constants, we wished to answer the questions: (1) what step or steps govern the kinetics giving rise to the observed $I-E$ data and (2) can the method be used to estimate k_1 and k_2 in systems with mixed kinetic control? In this paper, the simulation/regression technique is applied to elucidate the rds for reduction of 4-bromobiphenyl and 4-chlorobiphenyl by the electrogenerated phenanthridine anion radical.

Kinetic Models for $I-E$ Data

Explicit finite-difference methods or "digital simulations" are accurate and potentially general numerical tools for computing theoretical LSV curves for any electrode reaction. The most efficient simulations¹⁰⁻¹³ employ the expanding space grid, in which the width (Δx_i) of the i th space element in the simulation model increases exponentially (eq 7) as distance from the electrode

$$\Delta x_i = \Delta x_1 \exp[0.5(i-1)] \quad i = 1, 2, 3, \dots, n \quad (7)$$

increases. Our approach was previously described in detail for various electrode mechanisms.¹⁰ In it, model parameters retain dimensions corresponding to those of the experimental data. This avoids the problem¹⁴ of relating theoretical dimensionless currents and potentials to real experimental values. Normalization of I and E is unnecessary and generality is not sacrificed, since parameter values are computed with the correct dimensions by regression analysis of experimental $I-E$ data onto simulation models.

The digital simulation procedure involves setting up an expanded space grid around the spherical electrode for each small uniform time element. Events in the electrochemical experiment are simulated in a stepwise fashion: (1) initial conditions, (2) surface boundary conditions, (3) diffusion of reaction participants, and (4) homogeneous kinetics coupled to heterogeneous electron transfer. Formulation of steps 1-4 was identical with that described previously.¹⁰ Δx_1 was equal to $(D\Delta t/D^*)^{1/2}$, where D is the system diffusion coefficient, D^* is the dimensionless diffusion coefficient set equal to 0.45 as recommended for best accuracy,¹² and Δt was chosen to yield estimated relative errors <0.001 in concentrations. In the present application, D is the same for all diffusing species. Perturbations in concentrations caused by kinetics of homogeneous reactions coupled to charge transfer (eq 1) can be computed separately from changes in concentration from diffusion. Thus, the concentration C_i^S of any species S in the i th space element can be written

$$C_i^S = W_i^S + \Delta(S)_i \quad (8)$$

where $\Delta(S)_i$ is the change in concentration anticipated from homogeneous chemical kinetics and W_i^S is the concentration anticipated from diffusion.

The concentrations of A, B, and ArX can be computed from eq 8, using the chemical kinetics of Scheme I to obtain $\Delta(S)_i$ for each species. If we assume that eq 5 and 6 describe fast steps in Scheme I, the general kinetics (KG case) can be expressed¹⁵ in the simulation as:

$$\Delta(B)_i = \Delta t \{-2k_1 W_i^B W_i^{ArX} / [1 + (k_{-1}/k_2) W_i^A]\} \quad (9)$$

$$\Delta(A)_i = -\Delta(B)_i \quad (10)$$

$$\Delta(ArX)_i = \Delta t \{-k_1 W_i^B W_i^{ArX} / [1 + (k_{-1}/k_2) W_i^A]\} \quad (11)$$

$$\Delta(ArX^{\cdot-})_i = 0 \quad (12)$$

Equation 12 derives from a stationary-state assumption on $ArX^{\cdot-}$, valid for all practical conditions in LSV,⁹ and further justified

(5) Andrieux, C. P.; Blocman, C.; Dumas-Bouchiat, J. M.; Saveant, J. M. *J. Am. Chem. Soc.* **1979**, *101*, 3431-3441.

(6) Andrieux, C. P.; Saveant, J. M.; Zann, D. *Nouv. J. Chim.* **1984**, *8*, 107-116.

(7) (a) Electron transfer to Ar^{\cdot} is only by eq 4 in our simulations. For aromatic halides the Ar^{\cdot}/Ar^- standard potential is more positive than that of $ArX/ArX^{\cdot-}$ by at least 2 V. Thus, the rate constant for eq 4 is expected to be close to the diffusion limit. Under these conditions electron transfer from the electrode to Ar^{\cdot} can be neglected.^{7b} (b) Saveant, J. M.; Su, K. B. *J. Electroanal. Chem.* **1985**, *196*, 1-22.

(8) Andrieux, C. P.; Blocman, C.; Dumas-Bouchiat, J. M.; M'Halla, F.; Saveant, J. M. *J. Am. Chem. Soc.* **1980**, *102*, 3806-3813.

(9) Andrieux, C. P.; Blocman, C.; Dumas-Bouchiat, J. M.; M'Halla, F.; Saveant, J. M. *J. Electroanal. Chem.* **1980**, *113*, 19-40.

(10) Arena, J. V.; Rusling, J. F. *Anal. Chem.* **1986**, *58*, 1481-1488.

(11) Joslin, T.; Pletcher, D. *J. Electroanal. Chem.* **1974**, *49*, 171-186.

(12) (a) Feldberg, S. W. *J. Electroanal. Chem.* **1981**, *127*, 1-10. (b) Feldberg, S. W. *Electroanal. Chem.* **1969**, *3*, 199-296.

(13) Seeber, R.; Stefani, S. *Anal. Chem.* **1981**, *53*, 1011-1016.

(14) O'Dea, J.; Osteryoung, J.; Lane, T. *J. Phys. Chem.* **1986**, *90*, 2761-2764.

(15) Arena, J. V. Ph.D. Thesis, University of Connecticut, Storrs, CT, 1986.

here because of short lifetimes of haloaromatic anion radicals.⁶ Equation 12 dictates that diffusion of $\text{ArX}^{\cdot-}$ need not be considered.

There are two limiting cases⁹ of eq 9–11. When $k_{-1}C_A^* \gg k_2$ [C_A^* = bulk concentration], then $(k_{-1}/k_2)W_i^A \gg 1$, and eq 9 and 11 become

$$\Delta(B)_i = \Delta t \{-2(k_1 k_2 / k_{-1}) W_i^B W_i^{\text{ArX}} / W_i^A\} \quad (13)$$

$$\Delta(\text{ArX})_i = \Delta t \{-k_1 k_2 / k_{-1}\} W_i^B W_i^{\text{ArX}} / W_i^A \quad (14)$$

This corresponds to kinetic control of the reaction by decomposition of the anion radical $\text{ArX}^{\cdot-}$ (KC case) in eq 3. On the other hand, when $k_2 \gg k_{-1}C_A^*$, then $k_{-1}W_i^A/k_2 \ll 1$, the homogeneous electron transfer in eq 2 is the rds (KE case), and eq 9 and 11 are simplified to

$$\Delta(B)_i = \Delta t \{-2k_1 W_i^B W_i^{\text{ArX}}\} \quad (15)$$

$$\Delta(\text{ArX})_i = \Delta t \{-k_1 W_i^B W_i^{\text{ArX}}\} \quad (16)$$

Thus, in simulating the homogeneous kinetics of Scheme I, eq 9–12 can be used with eq 8 to compute the concentration of each diffusing species in each space element. However, when the simulation is coupled to nonlinear regression analysis, under conditions where eq 2 is the rds, no unique value of k_2 can be computed upon convergence since for any value of $k_2 \gg k_{-1}C_A^*$, $k_{-1}W_i^A/k_2$ will be approximately zero. Thus, when $k_2 \gg k_{-1}C_A^*$, eq 15 and 16 with k_1 as the only kinetic parameter must be used for proper convergence. Moreover, when decomposition of ArX is the rds, $k_2 \ll k_{-1}C_A^*$ and eq 9 and 11 are computationally equivalent to eq 13 and 14, respectively. In the latter equations k_1 and k_2 only appear as their product, and only their product can be obtained as a parameter in nonlinear regression analysis. Thus, only under mixed kinetic control of eq 2 and 3 can the general eq 9–11 be used to obtain simultaneous estimates of k_1 and k_2 , by assuming that k_{-1} is diffusion limited. It is necessary to have a regression/simulation program for each of the three kinetic situations, i.e. the two limiting cases (KC and KE) and the mixed kinetic (KG) case.

The digital simulations described above were used as subroutines to supply calculated LSV currents to a general nonlinear regression program employing the Marquardt method for convergence. Starting with the best initial guesses for model parameters, the regression algorithm systematically varies the parameters to find the global minimum of an error function, in the present case the sum of squares of the differences between measured and computed currents. The best values of the parameters are found at the minimum of the error function, called the point of convergence. Specific computational details are described elsewhere.^{10,16,18}

Experimental Section

Phenanthridine, 4-chlorobiphenyl, and 4-bromobiphenyl were from Aldrich Chemical Co. and were recrystallized two or more times from absolute methanol. Tetrabutylammonium iodide (TBAI) was from Aldrich and used as received. *N,N*-Dimethylformamide (DMF) was Burdick and Jackson "distilled-in-glass" grade. It was stored, dried, and purified as described previously.¹⁷

Electrochemical instrumentation, three-electrode cells, and procedures were the same as those reported previously.¹⁰ The working electrode was a spherical hanging-drop mercury electrode ($A = 0.0183 \text{ cm}^2$), the counter electrode was a platinum wire, and the reference was a Ag/AgI wire. Ohmic distortion of voltammograms was negligible after compensation of about 70% of the IR drop of the cell. All experiments were done at the ambient temperature of the laboratory (24 °C) and potentials were corrected and reported vs. SCE.

Nonlinear regression analysis was done in double precision with a general program based on the Marquardt algorithm^{16,18} in Fortran 77. The program was modified by writing the simulation model to be fit to the experimental data in a subroutine called YCALC. (The YCALC subroutines are available from the authors.) Programs were compiled by an IBM V.S. Fortran Compiler on an IBM 3081D computer. In the simulation models, all species involved were assumed to have equal diffusion coefficients. An upper limit of 1000 space elements could be used. However, when $W_n^A \geq 0.999C_A^*$ and $W_n^{\text{ArX}} \geq 0.999C_{\text{ArX}}^*$, then only n elements were used for that time unit in the simulation. The value of Δt was computed by dividing 0.0001 V by the scan rate (v).

The observed LSV current is composed of a Faradaic component (I_f) and a background component, the latter consisting of the current needed to charge the electrode double layer and to electrolyze minor impurities. In the present work, the background current was assumed to increase linearly as the potential became more negative, and the total calculated current (I_c) is given by

$$I_c = I_f + m(E' - E) + I' \quad (17)$$

In eq 17, I_f is computed from the simulation,¹⁰ m is the slope of the background current, and I' is the background current at an arbitrary fixed potential E' . The rate constant (k^0) for heterogeneous electron transfer to the catalyst was set at 10 cm s^{-1} . I' , m , and E^0 of the catalyst and D were parameters in all regression analyses. Initial guesses for I' and m were made from a linear regression on the base line of experimental voltammograms, choosing E' well before the rise of the catalytic current. Good initial estimates of D and E^0 were available from reversible voltammograms of the catalyst.¹⁰ For simulation of chemical kinetics, the KG model employed eq 9–12 in the YCALC subroutine, with kinetic parameters k_1 and k_2 . From standard potentials,⁴ the standard free energy for the back-electron-transfer reaction (eq 2) is on the order of -0.3 eV , and we assumed¹⁹ in all the simulation models that k_{-1} is at the average diffusion limit of $5 \times 10^9 \text{ M}^{-1} \text{ s}^{-1}$ for similar sized molecules²⁰ in DMF. For the KC case eq 10 and 12–14 were used, and the kinetic parameter in the regression is $k_1 k_2$. For the KE case eq 10, 12, 15, and 16 were used, with the kinetic parameter k_1 . Initial estimates of kinetic parameters were based on comparisons of catalytic increases in the cathodic LSV current with working curves,⁹ but only roughly approximate estimates were needed for good convergence.

Synthetic voltammograms were computed from the simulation models. When required, normally distributed noise (0.5% of peak current) was added as described previously.² Forty I - E pairs equally spaced on the E axis, from the foot of the rising portion of the curve to beyond the maximum current, were used for all nonlinear regression analyses. Evaluation of "goodness of fit" was by relative standard deviation of regression, by visual observation of randomness of deviation plots,¹⁰ and by a χ^2 test on residuals as described by Meites.²¹

Results

Preliminary tests of the simulation/regression analysis with pseudo-first-order electrocatalytic data from Nicholson–Shain current functions²² showed the validity of the method for this case. They also confirmed the necessity of a spherical diffusion model. For example, for theoretical data with $k_1 = 7.78 \text{ M}^{-1} \text{ s}^{-1}$, the regression program returned a value of $7.59 \text{ M}^{-1} \text{ s}^{-1}$ when the spherical correction was included in the data, but a value of $4.14 \text{ M}^{-1} \text{ s}^{-1}$ when the data were strictly from the linear diffusion function. The error from neglecting sphericity decreased as k_1 increased.¹⁵ For the KE case, dimensionless peak potentials and currents from the digital simulation were compared to values⁹ obtained by the Crank–Nicholson implicit finite-difference method.

(19) Miller, J. R.; Calcaterra, L. T.; Closs, G. L. *J. Am. Chem. Soc.* **1984**, *106*, 3047–3049.

(20) Kojima, H.; Bard, A. J. *J. Am. Chem. Soc.* **1975**, *97*, 6317–6324.

(21) (a) Meites, L. Manual for "The General Multiparametric Curve-Fitting Program CFT4", Computing Laboratory, Department of Chemistry, Clarkson University, 1976. (b) This test constitutes a statistical measure of randomness of the residuals.

(22) Nicholson, R. S.; Shain, I. *Anal. Chem.* **1964**, *36*, 707–723.

(16) (a) Marquardt, D. W. *J. Soc. Ind. Appl. Math.* **1963**, *11*, 431–441. (b) Christian, S. D.; Tucker, E. E. *Am. Lab. (Fairfield, Conn.)* **1982**, Sept, 31–36.

(17) Rusling, J. F.; Arena, J. V. *J. Electroanal. Chem.* **1985**, *186*, 225–235.

(18) Nonlinear Least Squares Program NLLSQ; CET Research Group, Norman, OK, 1981.

TABLE I: Comparison of Simulation Results ($\delta^c = 1$) for the KE Case to Published Results from the Crank-Nicholson Method

$RTk_1C^*_A/Fv$	$F(E^0 - E_p)/RT$		$I_p(RT)^{1/2}/FAC^*_A(DvF)^{1/2}$	
	ref 9 ^a	our work	ref 9 ^a	our work
		$\Delta t = 10$ ms		
0	1.3	1.17	0.45	0.491
0.2	1.8	1.95	0.70	0.694
2	1.7	1.56	1.2	1.25
20	0	0	1.4	1.44
		$\Delta t = 0.1$ ms		
200	-1.7	-1.56	1.3	1.40
2000 ^b	-3	-2.72	1.2	1.25
	0.5	0.78	0.9	1.12

^a Estimated from published graphs. ^b Two peaks occur under these conditions. The first corresponds to electrocatalysis, the second to diffusion-controlled reduction of catalyst. ^c $\gamma = C^*_{ArX}/C^*_A$.

Considering that these previously reported values were for planar diffusion, good agreement was obtained between the two sets of results (Table I). Characteristic double cathodic peaks⁹ at large values of the kinetic parameter were reproduced by the simulation.

Regressions of synthetic data onto the three kinetic models were used to further test the simulation/regression procedures (Table II). Both noise-free and noisy (0.5% of peak current) synthetic data were used. The noise level represents the approximate average noise in typical current measurements in electrocatalytic systems, as estimated in previous studies.^{2,10} Appropriate values of k_1 and k_2 for the three different kinetic situations were chosen from a published⁸ kinetic zone diagram describing conditions for the limiting cases. As reported previously for the KE case, the same convergence points and values for kinetic parameters were found even when initial guesses of these parameters were in error by two orders of magnitude. Excellent agreement between computed and expected values of the regression parameters, relative standard deviations of regression (RSD) <0.35% for the noisy data, and random residual or deviation plots (i.e. plots of $\{I_c - I(\text{meas})\}/SD$ vs. E) demonstrated the reliability of the computations. Correlation matrices computed by the regression program¹⁸ further confirmed the absence of correlation among parameters. These results (Table II) also illustrate that when the system is under mixed kinetic control, k_1 and k_2 can be evaluated simultaneously. However, the standard error in k_1 and k_2 is significantly greater in regression of the mixed kinetic data compared to k_1 determined from data in the KE region.

Synthetic data were also used to investigate the possibility of distinguishing between the three kinetic cases by analyzing the "goodness of fit" of the regression models. Data were evaluated

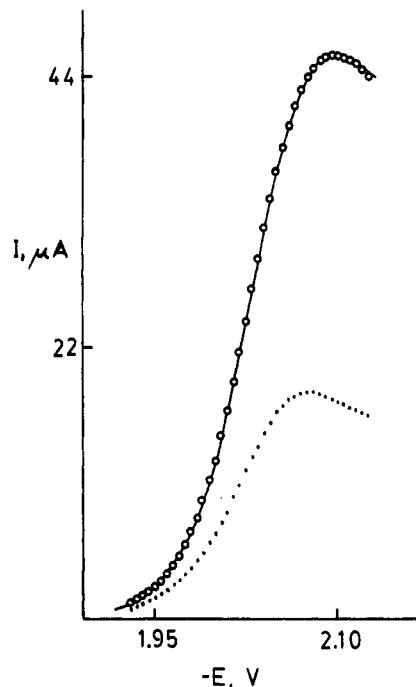


Figure 1. Linear-sweep voltammogram for 0.87 mM phenanthridine and 1.3 mM 4-BB in 0.1 M TBAI/DMF at 0.50 V s⁻¹. Solid line is best fit by simulation/regression method (KE model); circles are experimental data. Dotted line is LSV for phenanthridine alone computed by using regression parameters from the electrocatalytic data.

by regression onto the models in the order: (1) KC model; (2) KE model; (3) KG model. Regression onto the KG model was done last to avoid possible correlation between rate constants which occurs, as described previously, for data falling in the limiting regions. Regression onto the KC model was first to avoid long computation times found when the KE model was fit to data arising from the KC case. We illustrate the procedure for model testing by considering synthetic KG data with 0.5% I_p noise having the parameters in the second row of Table II. Background current (eq 17) was added with $m = 1 \mu\text{A}/\text{V}$ and $I' = 0.2 \mu\text{A}$. When the KC model was fit to these data, the deviation plot was considerably nonrandom, and an RSD of 0.55% was found. A second regression analysis onto the KE model gave a nonrandom deviation plot and a RSD of 0.92%. The nonrandom deviation plots indicate that neither model accurately described the data. As expected, when the KG model was fit to the data a random deviation plot and an RSD of 0.27% were found, confirming the mixed kinetics

TABLE II: Regression Analyses of Synthetic Voltammetric Data

$N,^a$ %	e^b	$10^5 D, \text{cm}^2 \text{s}^{-1}$	$-E^0, \text{V}$ vs. SCE	$10^{-4} k_1, \text{M}^{-1} \text{s}^{-1}$	$10^{-5} k_2, \text{M}^{-1} \text{s}^{-1}$	RSD ^c
KG Case						
0	-10/-10	1.00	1.500	5.00	3.00	5×10^{-6}
0.5	$\pm 10/\pm 10$	1.00	1.500	4.99 ± 0.64	3.04 ± 0.41	0.32
theory		1.00	1.500	5.00	3.00	
KE Case						
0	+10/+5	0.999	1.501	1.93		0.004
0.5	$\pm 10/\pm 5$	0.998	1.501	1.94 ± 0.03		0.34
theory		1.00	1.500	2.00		
KC Case						
					$10^{-9} k_1 k_2, \text{M}^{-1} \text{s}^{-2}$	
0	-10/-5	0.981	1.499		2.03	0.16
0.5	$\pm 10/\pm 5$	0.986	1.500		2.01 ± 0.03	0.34
theory		1.00	1.500		2.00	
0	+10/+5	1.00	1.500		6.40	0.0006
0.5	$\pm 10/\pm 5$	1.00	1.500		6.40 ± 0.04	0.29
theory		1.00	1.500		6.40	

^a Random noise as % I_p . For all synthetic data $C^*_A = C^*_{ArX} = 1 \text{ mM}$, $A = 0.0183 \text{ cm}^2$, $v = 0.2 \text{ V s}^{-1}$. ^b Percent error in initial parameters. ± 10 denotes three fits with errors of 10, 0, and -10. Number to right of slash is error in the initial value of E^0 . ^c Standard deviation of regression $\times 100\%$ divided by I_p .

TABLE III: Goodness of Fit of Selected Voltammetric Data to KC and KE Models

substrate	C_A^* , ^a mM	KC model		KE model	
		RSD, %	χ^2	RSD, %	χ^2
4-CB ^a	2.1	0.58	7.4	0.36	3.10
		0.55	16.0	0.44	9.25
	0.96	0.57	11.3	0.35	0.23
		0.48	16.0	0.44	1.26
		0.49	7.4	0.45	3.10
4-BB ^a	0.87	0.46	4.3	0.40	0.02
		0.57	3.1	0.42	0.23
		0.44	2.1	0.49	0.03
		0.45	5.8	0.46	0.03

^aSubstrate concentration 1.3 mM, catalyst was phenanthridine.

which gave rise to the data. This procedure led to similar correct decisions when data representing the two limiting cases were analyzed. These results suggested the possibility of distinguishing among the three kinetic cases from experimental data in the absence of unforeseen systematic error when the random noise level is $\leq 0.5\%$ of the peak current.

Experimental LSV data for the reduction of 4-bromo- (4-BB) and 4-chlorobiphenyl (4-CB) using phenanthridine as catalyst were analyzed by the above scheme. Comparison of results from regression onto the KC and KE models for 4-CB shows that in all cases smaller RSD's (Table III) are found for the KE model. However, small nonrandom features were observed in deviation plots for both models. This was not surprising since similar features were found even for voltammograms of compounds undergoing only heterogeneous electron transfer.¹⁰ They are probably caused by minor systematic errors either in the model or in the measuring system. Nevertheless, these small deviations complicated visual examination of residuals in assessing which model gave the best fit to the data. To facilitate this decision we further analyzed residuals with a χ^2 test²¹ on the residuals, which had been much more discriminating in comparing closely related models for a different electrochemical system.²³ Smaller values of χ^2 for every set of data (Table III) indicated a greater degree of randomness in residuals for the KE model. Thus, the KE model gave the best fit, confirming eq 2 as rds. Regression analyses did not converge when the KG model was used. The mean k_1 for 4-CB from the regression/simulation method, as reported previously,¹⁰ was $(1.42 \pm 0.12) \times 10^3 \text{ M}^{-1} \text{ s}^{-1}$. On the other hand, the average $k_1 k_2$ from the KC model was $(4.3 \pm 1.3) \times 10^8 \text{ M}^{-1} \text{ s}^{-2}$. From analysis of noisy synthetic data (Table II), the relative precision of kinetic parameters is expected to be the same for KC and KE regressions if they are the correct models. Thus, the poorer relative standard deviation (30%) of $k_1 k_2$ for regression onto the KC model supports the correctness of the KE model, which gave a relative standard deviation of 8.5% for k_1 .

Data for 4-BB presented a minor problem in the negative potential range, since reduction potentials of the catalyst and substrate were closer together in this case. Possibly related to such complications, in two sets of data at 0.50 V s^{-1} RSD values were within experimental error of one another, although in another set of data RSD for the KE model was clearly smaller (Table III). The χ^2 test, however, showed that deviation plots for the KE model were more random in all cases. Excellent agreement between computed and experimental values of currents were found (Figure 1). Regression analyses did not converge when the KG model was used. Model testing of data at 0.20 V s^{-1} was complicated by systematic deviations in the negative potential range, probably caused by a small contribution to the current from direct substrate reduction. However, analyses of nine sets of $I-E$ data (Table IV) with the KE model for the 4-BB system showed acceptable precision for regression parameters. Further support for the KE model comes from comparing precisions of kinetic parameters and their dependence on C_A^* , as discussed below.

TABLE IV: Parameters from Nonlinear Regression Analysis of Voltammograms for Reduction of 4-Bromobiphenyl with Phenanthridine as Catalyst

trial ^a	$10^5 D$, $\text{cm}^2 \text{ s}^{-1}$	$-E^0$, V vs. SCE	$10^{-4} k_1$, $\text{M}^{-1} \text{ s}^{-1}$	RSD, %
$C_A^* = 0.87 \text{ mM}$				
1	2.0	2.047	3.72	0.49
2	2.1	2.047	3.19	0.46
3	2.2	2.041	2.74	0.42
4	2.1	2.069	6.62	0.48
5	2.1	2.046	7.42	0.95
$C_A^* = 1.7 \text{ mM}$				
6	2.7	2.066	5.14	0.97
7	2.7	2.071	5.30	0.69
8	2.8	2.082	6.77	0.57
mean	2.3	2.059	5.11	0.63
s	0.3	0.015	1.76	0.22

^aConcentration was 1.3 mM for 4-BB. Trials 1-3 used data at $v = 0.50 \text{ V s}^{-1}$ digitized at 5-mV intervals between -1.930 and -2.125 V vs. SCE. Trials 4-8 on data at $v = 0.20 \text{ V s}^{-1}$ at 5-mV intervals between -1.930 and -2.110 V.

Discussion

Comparisons of regression analyses onto the three kinetic models clearly show that electron transfer between the initially formed anion radical of phenanthridine and the halobiphenyls (eq 2) is the rds in the reduction of 4-CB and 4-BB. Further evidence employs the prediction that, for the KE case, constant values of k_1 should be obtained when catalyst concentration is varied. However, if the KE mechanism is incorrectly assumed for KC data, computed values of k_1 will vary with catalyst concentration.^{5,8,9} Conversely, if the KC model is incorrectly assumed for KE data, $k_1 k_2$ will vary with catalyst concentration. Mean values of k_1 for 4-BB at 0.87 and 1.7 mM phenanthridine were 4.7×10^4 and $5.7 \times 10^4 \text{ M}^{-1} \text{ s}^{-1}$, respectively, while values of $k_1 k_2$ from the KC model were 4.9×10^{10} and $9.5 \times 10^{10} \text{ M}^{-1} \text{ s}^{-2}$. Moreover, the overall mean of $k_1 k_2 = (6.6 \pm 5.2) \times 10^{10} \text{ M}^{-1} \text{ s}^{-2}$ for 8 data sets had much worse precision than the $k_1 = (5.1 \pm 1.8) \times 10^4 \text{ M}^{-1} \text{ s}^{-1}$. Values¹⁰ of k_1 for 4-CB at 0.96 and 2.1 mM catalyst averaged 1.43×10^3 and $1.40 \times 10^3 \text{ M}^{-1} \text{ s}^{-1}$, respectively, whereas (KC model) $k_1 k_2$ were 3.3×10^8 and $5.2 \times 10^8 \text{ M}^{-1} \text{ s}^{-2}$ at these two concentrations. Thus, better precision and agreement of kinetic parameters when C_A^* is varied confirms eq 2 as the rds for reduction of both halobiphenyls. This is the same rds found for halobenzenes and pyridines.⁵ The homogeneous electron-transfer step is always slower than decomposition of the halobiphenyl anion radical in DMF. Thus, any stabilizing effect of the phenyl group in the anion radical is not large enough to slow its decomposition sufficiently for eq 3 to become the rds.

Values of k_1 , D , and E^0 determined from regression analyses of the 4-BB data (Table IV) had relative standard deviations of 34%, 13%, and 0.7%, respectively. Values of D and E^0 can be compared with independent determinations to further assess the validity of the results. The digital simulation model assumes equal diffusion coefficients, and the value obtained is in reasonable agreement with those estimated from voltammograms of biphenyl ($1.5 \times 10^{-5} \text{ cm}^2 \text{ s}^{-1}$)¹⁷ and phenanthridine ($1.9 \times 10^{-5} \text{ cm}^2 \text{ s}^{-1}$).²⁴ E^0 is also in good agreement with the value of -2.040 V vs. SCE (corrected from Ag/AgI) obtained from voltammograms of phenanthridine under identical conditions.¹⁵ Considering the potential drift of the Ag/AgI reference electrode in DMF,¹⁵ agreement with an earlier reported value⁴ of -2.005 V is satisfactory.

For the 4-CB reaction with phenanthridine anion radical, k_1 of $(1.42 \pm 0.12) \times 10^3 \text{ M}^{-1} \text{ s}^{-1}$ by the simulation/regression method was in excellent agreement with the value of $(1.6 \pm 0.6) \times 10^3 \text{ M}^{-1} \text{ s}^{-1}$ from the pseudo-first-order method.⁴ The value of k_1 for the 4-BB system (Table IV) is about tenfold larger than

(23) Rusling, J. F.; Brooks, M. Y.; Scheer, B. J.; Chou, T. T.; Shukla, S. S.; Rossi, M. *Anal. Chem.* **1986**, *58*, 1942-1947.

(24) Connors, T. F. M.S. Thesis, University of Connecticut, Storrs, CT, 1983.

the previously reported value of $(0.6 \pm 0.7) \times 10^4 \text{ M}^{-1} \text{ s}^{-1}$. However, the latter value obtained under pseudo-first-order conditions is subject to larger errors compared to 4-CB because the peak potential (E_p) of 4-BB is much closer to the E^0 of the catalyst. As mentioned in the Introduction, in the pseudo-first-order method the catalytic current is separated from background current for direct reduction of substrate by nonlinear regression. Values of k_1 are then computed from their proportionality to $(I_c/I_d)^2$, where I_c is the limiting catalytic current, and I_d is the peak current of the catalyst alone. Analysis of errors² in the pseudo-first-order method predict that, under conditions of significant overlap of catalytic and background $I-E$ curves, a decrease in $E^0 - E_p$ of 40 mV leads to about a fourfold increase in relative standard error in k_1 . E_p for 4-BB is 42 mV more positive than for 4-CB,¹⁷ and for this reason the pseudo-first-order-derived k_1 for 4-BB has significantly worse precision than that of 4-CB. In fact, k_1 of 4-BB/phenanthridine approaches the upper limit that can be estimated by the pseudo-first-order method.

As an additional check on the 4-BB system, k_1 was estimated from a working curve⁹ of $(F/RT)(E^0 - E_{p/2})$ vs. $\log [RTC^*_A k_1/Fv]$, where $E_{p/2}$ is the half-peak potential of the catalytic $I-E$ curve. This method gave $7 \times 10^4 \text{ M}^{-1} \text{ s}^{-1}$, in good agreement with the second-order simulation/regression (Table IV). Further evidence of the validity of that value is that k_1 values of a series of catalysts reacting with 4-BB were generally about 10-fold greater than for 4-CB.⁴ The present value also better follows the trend⁴ of increasing k_1 with a decrease in $E^0 - E_p$.

Thus, the second-order simulation/regression method appears to extend the upper limit of k_1 determinations by at least an order of magnitude over the pseudo-first-order method. Poorer precision for 4-BB than for 4-CB suggests a decrease in precision as k_1 increases, especially in cases where the substrate is reduced at potentials only slightly more negative than the catalyst. Precision should be optimized for such systems with higher k_1 values by using smaller concentrations of substrate. In such cases, confirmation of the rds by examining the influence of C^*_A on fitted kinetic parameters is highly recommended.

Recent results in our laboratory²⁵ showed that, for systems in which the substrate is reduced at potentials much more negative

than E^0 of the catalyst, the upper limit of k_1 is much greater than the value found for the phenanthridine/4-BB system. Specifically, the regression/simulation was applied to reduction of 1,2-dibromobutane by electrogenerated vitamin B_{12s} [Co(I) form]. For this system, direct reduction of substrate occurs about 0.8 V more negative than the E^0 of the catalyst. Moreover, no substrate anion radical exists, eq 3 was formally considered a very fast step, and the reaction of Co(I) and substrate is the rds. Analysis of voltammetric data at scan rates between 10 and 25.6 V s⁻¹ gave²⁵ a rate constant of $(6.1 \pm 2.2) \times 10^6 \text{ M}^{-1} \text{ s}^{-1}$. This application required minor changes in the simulation to include unequal diffusion coefficients of substrate and catalyst, planar diffusion, and smaller values of the heterogeneous rate constant for electron transfer. Since the ratio (d) of diffusion coefficients of substrate:catalyst was correlated with k_1 in the regression analysis, d was fixed at an experimentally estimated value. Successful estimation of k_1 in this case can be used with the dimensionless kinetic parameter $\lambda = (RT/F)C^*_A(k_1/v)$, which governs relative catalytic current,⁹ to obtain an upper limit of estimable k_1 . For the 1,2-dibromobutane/vitamin B_{12s} system, the largest λ used for regression was 15.4. Thus, assuming good data can be obtained at $v = 50 \text{ V s}^{-1}$ and $C^*_A = 0.3 \text{ mM}$ for $\lambda = 15.4$ yields an estimated upper limit on k_1 of $10^8 \text{ M}^{-1} \text{ s}^{-1}$, subject to the limitation of fixed d .

In summary, the method to elucidate kinetic behavior of homogeneous electrocatalytic reactions is general and applicable to any catalytic system following the assumptions, offering to provide more precise and accurate values of rate constants. This is also important in the separate context of estimating thermodynamic parameters from free energy relationships for compounds which undergo slow electron transfer at electrodes.^{4,5} In addition, when mixed kinetic control can be attained, determination of both k_1 and k_2 from the same experiment is possible. Assumptions of the simulation models are easily modified to apply to slightly different systems.

Acknowledgment. This work was supported by U.S. PHS Grant No. ES03154 awarded by the National Institute of Environmental Health Sciences.

Registry No. 4-CB, 2051-62-9; 4-BB, 92-66-0; phenanthridine, 229-87-8; phenanthridine anion radical, 34518-98-4.

(25) Connors, T. F.; Arena, J. V.; Rusling, J. F., unpublished results.

Temperature and Pressure Dependence of the Rate Constant for the Addition of H to C₂H₄

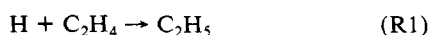
Phillip D. Lightfoot and Michael J. Pilling*

Physical Chemistry Laboratory, Oxford, OX1 3QZ, U.K. (Received: October 10, 1986; In Final Form: February 9, 1987)

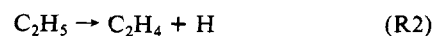
The rate constant for the reaction $\text{H} + \text{C}_2\text{H}_4 \rightarrow \text{C}_2\text{H}_5$ has been measured, as a function of temperature and pressure, over the ranges $285 \leq T/\text{K} \leq 604$ and $50 \leq p/\text{Torr} \leq 600$, in a helium diluent, by laser flash photolysis/resonance fluorescence. The limiting high- and low-pressure rate constants, $k_1^\infty(T)$ and $k_1^0(T)$, were obtained from nonlinear least-squares fits to the data using the Troe factorization procedure, with a transition-state model proposed by Hase and Schlegel. The values for $k_1^\infty(T)$ were combined with previous data, obtained at lower temperatures, to give an overall Arrhenius expression: $k_1^\infty(T) = (4.39 \pm 0.56) \times 10^{-11} \exp\{-(1087 \pm 36)/T\} \text{ cm}^3 \text{ molecule}^{-1} \text{ s}^{-1}$, where the uncertainties represent 95% confidence limits, as returned directly from the data analysis. The falloff parameters obtained from the fits to the experimental data were employed to provide estimates of $k_1(P,T)$ over the temperature range 600–1200 K.

Introduction

The addition of hydrogen atoms to ethylene



and the reverse decomposition



are of central importance in the high-temperature pyrolysis of alkanes and, in particular, of ethane, especially at the high conversions which pertain in industrial crackers. (R2) is also important in combustion. (R1) has been widely studied at low